Odorant-Induced Currents in Intact Patches from Rat Olfactory Receptor Neurons: Theory and Experiment

Pauline Chiu, Joseph W. Lynch,[†‡] and Peter H. Barry
School of Physiology and Pharmacology, University of New South Wales, Sydney 2052 and Neurobiology Division, Garvan Institute for Medical Research, Darlinghurst, NSW, 2010, Australia

ABSTRACT Odorant-induced currents in mammalian olfactory receptor neurons have proved difficult to obtain reliably using conventional whole-cell recording. By using a mathematical model of the electrical circuit of the patch and rest-of-cell, we demonstrate how cell-attached patch measurements can be used to quantitatively analyze responses to odorants or a high (100 mM) K^+ solution. High K^+ induced an immediate current flux from cell to pipette, which was modeled as a depolarization of ~52 mV, close to that expected from the Nernst equation (56 mV), and no change in the patch conductance. By contrast, a cocktail of cAMP-stimulating odorants induced a current flux from pipette into cell following a significant (4–10 s) delay. This was modeled as an average patch conductance increase of 36 pS and a depolarization of 13 mV. Odorant-induced single channels had a conductance of 16 pS. In cells bathed with no Mg^{2+} and 0.25 mM Ca^{2+}, odorants induced a current flow from cell to pipette, which was modeled as a patch conductance increase of ~115 pS and depolarization of ~32 mV. All these results are consistent with cAMP-gated cation channels dominating the odorant response. This approach, which provides useful estimates of odorant-induced voltage and conductance changes, is applicable to similar measurements in any small cells.

INTRODUCTION

Olfactory sensory transduction is mediated by olfactory receptor neurons (ORNs), which line the nasal epithelium and project numerous cilia into the mucous lining of the airway. The cilia contain odorant-sensitive G-protein-coupled receptors and the other molecular elements of the olfactory signal transduction pathway. When stimulated by odorants, these receptors induce the activation of either the cAMP or the inositol trisphosphate (IP_3) second messenger pathways (Reed, 1992; Ache and Zhainazarov, 1995). These second messengers then modulate the activity of a variety of membrane ion channels, thereby altering the pattern of neuronal activity (Dionne and Dubin, 1994; Ache and Zhainazarov, 1995).

Perhaps the most ubiquitous of these channels is the olfactory cyclic nucleotide-gated (CNG) cation channel, which was originally described in the frog (Nakamura and Gold, 1987). Under physiological external calcium concentrations, these channels are selective mainly for calcium (Frings et al., 1995). Calcium entry through these channels activates a Cl^- conductance (Kleene, 1993; Kurahashi and Yau, 1993), which amplifies cellular depolarization (Lowe and Gold, 1993). Both CNG channels and Ca^{2+}-gated chloride channels are present in mammalian olfactory neurons and are both involved in the cellular response to odorants (Frings et al., 1992; Lowe and Gold, 1993). Other examples of second messenger-modulated ion channels from the olfactory neurons of a variety of species include: IP_3-gated Ca^{2+} channels (Fadool and Ache, 1992; Okada et al., 1994; Hatt and Ache, 1994), IP_3-gated nonselective cation channels (Schild et al., 1995), IP_3-gated K^+ channels (Morales et al., 1994), Ca^{2+}-activated cation channels (Schild and Lischka, 1994), Na^+-activated K^+ channels (Zhainazarov and Ache, 1995) and voltage-gated Na^+ and K^+ channels (Dubin and Dionne, 1993, 1994; Pun et al., 1994). However, it is not yet certain which of these are expressed in mammalian olfactory neurons, and if they are, whether they contribute significantly to the odorant response.

We are interested in characterizing how odorants modulate the activity of ion channels in mammalian olfactory neurons. Although numerous reports testify to the relative ease of obtaining odorant responses from crustacean and amphibian olfactory receptor neurons (reviewed in Dionne and Dubin, 1994), there are as yet few reports describing odorant responses in acutely isolated mammalian olfactory neurons (Lowe and Gold, 1993; 1995). The difficulty of recording from isolated mammalian neurons appears at least partly due to their extremely small size and fine cilia. The cilia, with diameters near 0.1 μM, are difficult to visually resolve and may easily be disrupted during dissociation. Furthermore, in our hands, odorant responses of rat olfactory neurons maintained in the whole-cell recording configuration are washed out rapidly.

Therefore, the first aim of this study was to determine whether cell-attached recording could yield reliable odorant responses from acutely dissociated adult rat olfactory receptor neurons. The second aim was to determine the type of information that can be derived from these data by use of an

Received for publication 2 October 1996 and in final form 25 November 1996.

[‡]Dr. Lynch's current address is now: Department of Physiology and Pharmacology, The University of Queensland, St. Lucia, Qld 4072, Australia.

Address reprint requests to Professor Peter H. Barry, School of Physiology and Pharmacology, University of New South Wales, Sydney 2052, Australia. Tel.: 61-2-9385-1101; Fax: 61-2-9385-1099; E-mail: p.barry@unsw.edu.au.

0006-3495/97/03/1442/16 $2.00

appropriate electrical model of the cell and patch and realistic minimal assumptions. We demonstrate that the magnitudes of the odorant-induced changes in voltage and conductance can be estimated with a fairly high degree of confidence, thus providing a basis for future studies aimed at investigating the ionic bases of such responses. This approach is also applicable to the analysis of similar measurements in any small, high-resistance cells.

MATERIALS AND METHODS

Cells were obtained from adult female Wistar rats using a method described previously (Lynch and Barry, 1991a). Cells were bathed in general mammalian Ringer's solution (GMR) containing (in mM): 140 NaCl, 5 KCl, 2 $CaCl_2$, 1 $MgCl_2$, 10 HEPES, and 10 glucose. This was then titrated to a pH of 7.4 with 1 M KOH and resulted in $[K]_o$ = 10.1 mM. Patch pipettes were constructed with a resistance of 3–8 MΩ. They were filled with the following solution (in mM): 115 KCl, 20 KF, 11 EGTA, and 10 HEPES. This solution was titrated to pH 7.2 with 1 M NaOH. Currents were recorded using a List EPC-7 patch clamp amplifier and recorded continuously onto Beta video tape using a digital audio processor and Sony beta video cassette recorder modified according to Bezanilla (1985). All experiments were performed at room temperature (20–22°C). Recordings were later filtered at 1 kHz, digitized at 2.5 kHz, and analyzed using the software package PNSCROLL (Barry and Quartararo, 1990). Data are expressed as mean ± SEM.

All measurements were performed on cells maintained in the cell-attached patch-clamp configuration (Fig. 1 *C*). Stimulus solutions were applied to cells by pressure ejection from a puffer pipette placed within 20–30 μm of the cell. A Picospritzer (General Valve Corp.) was used to control the magnitude and duration of the stimulus. Cells that responded in any way to pressure ejection of GMR solution were excluded from analysis.

To observe the effect of cell depolarization in a cell-attached patch, a high K^+ solution was applied, containing (in mM): 100 KCl, 45 NaCl, 2 $CaCl_2$, 1 $MgCl_2$, and 10 HEPES. A liquid junction potential of −2.8 mV between the high KCl solution adjacent to the cell membrane and the bulk GMR solution was calculated using the program *JPCalc* (Barry, 1994). No such corrections were necessary for the odorant solutions. All solutions were titrated to pH 7.4 using 1 M KOH. The odorant solution was prepared on the day of the experiment by dissolving the following odorants in control solution to make a concentration of 1 mM of each odorant: cineole, *n*-amyl acetate, methyl salicylate, limonene, and α-pinene. All these odorants have been shown to selectively activate the cAMP second messenger pathway (Pace et al., 1985).

RESULTS

To obtain the most information from the data presented below, detailed theoretical analyses have been developed in Appendices A and B. The aim of these appendices has been to correctly account for the electrical circuit of the patch and the rest-of-cell in these small, high-input resistance cells under conditions of both high K^+-induced depolarization and odorant stimulation. Where appropriate, the most relevant equations are also listed in the text.

Depolarization with high K^+ solution

The effects of odorants on cell-attached patches may be due to either the depolarization of the cell, second messenger-mediated changes in patch ion channel activity, or both. Hence, before studying the odorant response, it was necessary to dissociate these effects by examining the response of a cell-attached patch to depolarization by a high (100 mM) K^+ solution. An elevated $[K]_o$ of 10 mM was used in the standard GMR solution to induce a slight cell depolarization to ensure that voltage-gated channels remained inactivated upon further depolarization (Lynch and Barry, 1991a,b; Rajendra et al., 1992). Whereas a control GMR application elicited no response when applied via a puffer pipette (Fig. 1 *A*), the high K^+ solution elicited an outward current across the patch into the pipette as shown in Fig. 1 *B*. The latency to the onset of the response was <1 s after initiation of the response. The response was not accompanied by any change in current noise level. Measurements of both the initial baseline current and the outward response current were made at a series of pipette potentials and plotted as shown in Fig. 1 *D*.

Appendix A describes the response of a cell and patch to

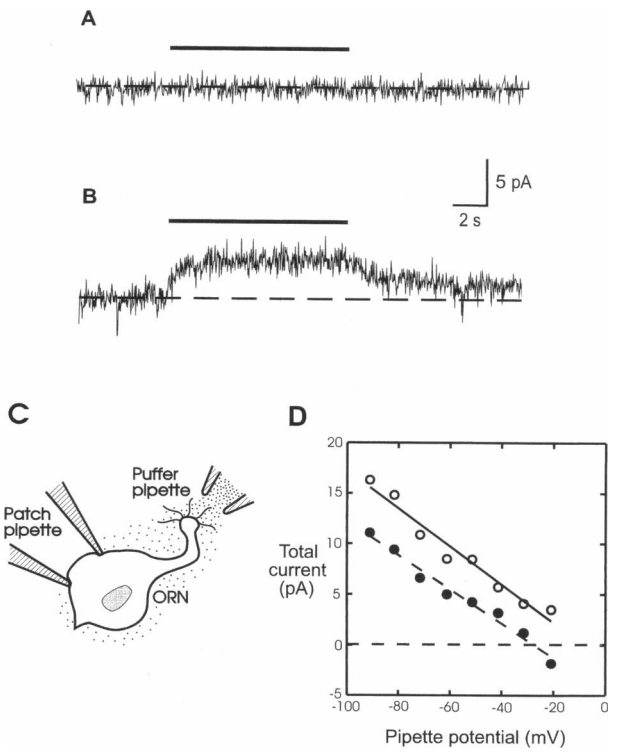

FIGURE 1 Pressure ejection of solutions onto cell-attached patches. Lines above each trace correspond to the duration of pressure ejection. (*A*) The application of the control solution (glucose-free GMR) onto a cell-attached patch for 10 s does not produce any change in the baseline current or noise. (*B*) The application of the high K^+ solution generates an outward current from the cell across the patch into the pipette. (*C*) The experimental set-up showing a schematic diagram of an isolated olfactory receptor neuron (ORN), which has been patch-clamped in the cell-attached patch configuration, with a puffer pipette from which solution can be perfused around the ORN. (*D*) A graph displaying the current values at various pipette potentials before (●) and after (○) application of the high K^+ solution. The upward shift of the points and the maintenance of the same slope means that application of K^+ does not greatly alter the resistance of the patch. The increase in current across the patch at V_p = 0, $\Delta I_p(0)$, was estimated to equal 3.0 pA.

perfusion of the cell by a high K^+ solution. With the assumption that the reversal potential for the membrane patch, $E_p \approx 0$ (see below and Appendix A; Eqs. A24–A26), the following equation may be used to describe these data:

$$I_p = I_p(0) - V_p/R_t \quad (1)$$

where

$$I_p(0) = E_o/R_{cell} \quad (2)$$

and

$$1/R_t = [1/R_{cell}] + [1/R_s] \quad (3)$$

with

$$R_{cell} = R_o + R_p \quad (4)$$

where I_p is the absolute pipette current recorded by the patch clamp amplifier, V_p is the pipette potential, $I_p(0)$ is the pipette current when $V_p = 0$, and R_t is the total resistance between the tip of the patch pipette and ground. R_t consists of two major parallel components (see Fig. A1): R_s, the resistance of the seal between pipette and membrane, and R_{cell}, the total resistance through the cell from pipette to bathing solution. R_{cell} is comprised of R_p in series with the rest-of-cell resistance, R_o. In turn, R_p consists of the background resistance of the patch in parallel with the resistance of any open ion channels within it. Rest-of-cell properties (e.g., resistance or conductance) in this paper refer to the properties of the entire cell membrane, except for that portion circumscribed by the patch pipette. The total resistance, R_t, is measured as the total change in current passing through the pipette for a given change in pipette potential.

In three cell-attached patches, R_t varied between 4.8 and 5.9 GΩ, with a mean of 5.2 ± 0.3 GΩ. Exposure to high K^+ solution did not significantly change this value (Table 1). At a pipette potential of 0 mV, the average value of I_p [defined as $I_p(0)$] was measured to be −3.5 ± 0.8 pA ($n = 3$) before high K^+ solution exposure, and this increased significantly to −1.1 ± 0.6 pA ($n = 3$) in the presence of high K^+ solution (Table 1).

With minimal assumptions, the above values of R_{cell} and $I_p(0)$ can enable us to estimate the shift in cell potential, V_{cell}. V_{cell}, in turn, can be related to the shift in the reversal potential, E_o, for the resting K^+ channels, to the value required to produce the observed outward current. The main assumptions are estimates of reasonable values for the reversal potential of the patch, E_p, and the K^+ equilibrium potential, E_K, between the cell and the external solution. The first value may be reasonably approximated as zero, provided that there is little or no K^+ concentration gradient across the patch membrane. The second can be approximated using the reasonable assumption that the cell is predominantly permeable to K^+ at rest. The only other assumption is that $R_p \gg R_o$, which is expected since the patch area is a small fraction of the whole cell area. In similar experiments, Lynch and Barry (1989) previously estimated this ratio to be between 10 and 100. However, as may be seen in Table 1, varying this value over a wide range (5–100) has very little impact on the values of the parameters of interest.

Before application of the high K^+ solution, the total cell resistance, R_{cell}, can be estimated using Eq. 2 as follows. Assuming a value of ~−65 mV for E_o before the application of the KCl solution (given $[K]_o = 10$ mM; with E_o estimated as −67 mV for $P_{Na}/P_K = 0$ and −63 mV for $P_{Na}/P_K = 0.01$), the value of R_{cell} may be estimated from Eq. 2 as ~18.8 ± 6.9 GΩ. The high K^+ solution may also be expected to change both E_o and R_{cell}. Defining these new values with a prime, it is shown in the derivation in Appendix A that Eqs. 1 and 2 now become:

$$I_p = I_p(0)' - V_p/R_t \quad (5)$$

Again, with the definition that $I_p = I_p(0)'$, when $V_p = 0$,

$$I_p(0)' = E_o'/R_{cell}' \quad (6)$$

and the total conductance, G_t, can be deduced from Eq. 5 from a plot of I_p against V_p, since:

$$-(dI_p/dV_p)' = 1/R_t' = [1/R_{cell}'] + [1/R_s] \quad (7)$$

Hence, the new value of the reversal potential of the resting channels, E_o', is given by:

$$E_o' = I_p(0)' \times R_{cell}' \quad (8)$$

Since R_t' displayed no significant reduction in the presence of high K^+ solution, it can be concluded that the patch contained no depolarization-activated channels. Even if R_o decreased sharply with depolarization due to the activation

TABLE 1 KCl perfusion experiments in GMR solutions

	Control resting situation						KCl perfusion situation							
Cell No.	$I_p(0)$ (pA)	E_o (mV)	V_{cell} (mV; $\alpha = 10$)	V_{cell} (mV; $\alpha = 100$)	R_{cell} (GΩ)	R_t (GΩ)	R_t' (GΩ)	R_{cell}' (GΩ)	$I_p(0)$ (pA)	$\Delta I_p(0)$ (pA)	E_o' (mV)	V_{cell}' (mV; $\alpha = 5$)	V_{cell}' (mV; $\alpha = 10$)	V_{cell}' (mV; $\alpha = 100$)
2112	−1.68	−65	−59.1	−64.4	38.8	4.78	4.34	21.4	0.43	2.10	9.13	7.61	8.3	9.0
2312B	−4.15	−65	−59.1	−64.4	15.7	4.93	4.89	15.3	−2.03	2.15	−30.6	−25.5	−27.9	−30.3
2212	−4.62	−65	−59.1	−64.4	14.1	5.94	5.31	11.0	−1.58	3.05	−17.3	−14.4	−15.8	−17.2
Avr	−3.48	−65	−59.1	−64.4	22.8	5.21	4.85	15.9	−1.05	2.43	−12.9	−10.8	−11.8	−12.8
SEM	0.79	0	0.0	0.0	6.91	0.31	0.24	2.6	0.65	0.27	10.1	8.4	9.2	10.0

These are the results of an analysis of intact patch measurements before and during high KCl perfusion, using the equations derived in Appendix A.

of voltage-gated channels elsewhere in the cell or to increases in external $[K^+]$, this change would not be reflected as a large change in R_t, as long as the resistance of the patch, R_p, is significantly greater than the resistance of the rest-of-cell. The new average value of $I_p(0)'$ was -1.05 ± 0.6 pA with R_{cell} changing from 22.8 ± 6.9 GΩ to an R'_{cell} of 15.9 ± 2.6 GΩ. Now, from an average of the product of $I_p(0)$ and R_{cell} for each of the cells, the estimated change in E_o would be from -65 mV to a new value, E_o, of -12.9 ± 10.1 mV (see Table 1). Thus, the mean shift in the reversal potential is $+52 \pm 10$ mV. The theoretically predicted maximum depolarization, ΔE_o, arising from application of the high K^+ solution, can be estimated using the Nernst equation

$$\Delta E_m = (2.303\ RT/F) \cdot \log_{10}([K^+]_{perf}/[K^+]_{bath}) \quad (9)$$

with $[K^+]_{perf}$ referring to the high K^+ concentration (105 mM) of the perfused solution around the cell and $[K^+]_{bath}$ to the original bathing solution (10 mM). Assuming complete perfusion of the cell by the high K^+ solution, the theoretically predicted depolarization using the Nernst equation should be $\sim +59$ mV plus a liquid junction potential correction of -2.8 mV (see Methods) $\approx +56$ mV. The close agreement between this value and the prediction of our model with our measurements ($+52 \pm 10$ mV) establishes the validity of this intact patch method for quantitating membrane potential changes.

Effect of odorant application in GMR

Odorant responses in cell-attached patches were observed in 5 of 30 cells in GMR, although only 4 were used for full data analysis. In each of the responsive cells, the application of odorant solution for 20 s resulted in a dramatic increase in current noise and a current flux out of the pipette and into the cell. A range of responses obtained from three different cells is shown in Fig. 2 *A*. The latency between the commencement of stimulus and onset of the response varied between 4.3 and 10.9 s. These odorant responses contrasted sharply with those observed with high K^+ solution, in which 1) the latency to onset of the response was very short; 2) the direction of the current was in the opposite direction; and 3) there was no significant increase in noise.

The mean R_t before odorant application was 3.7 ± 1.3 GΩ ($n = 4$), determined as $-dV_p/dI_p$. In the same four cells, the mean $I_p(0)$, the pipette current at zero pipette potential, before odorant application was -5.3 ± 2.2 pA and the average net increase in current after odorant application, $\Delta I_p(0)$, was -0.77 ± 0.10 pA.

Defining G_{cell}, before, and G^*_{cell}, after, odorant application by:

$$G_{cell} \equiv 1/R_{cell} \quad (10)$$

$$G^*_{cell} \equiv 1/R^*_{cell} \quad (11)$$

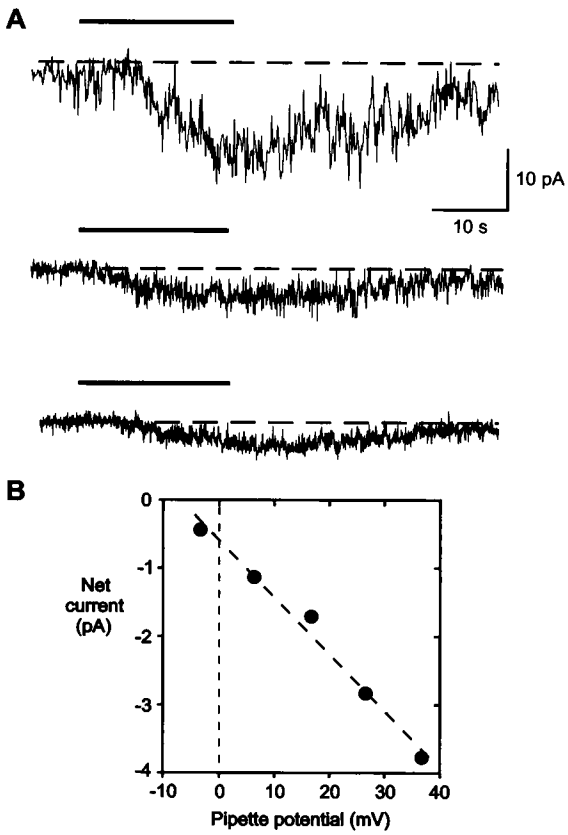

FIGURE 2 The current response obtained from different cells during a 20-s application of the odorant mixture in a bath containing GMR that included 2 mM Ca^{2+} and 1 mM Mg^{2+}. An inward current was generated in all responsive cells but with considerable variation in appearance. The latency of the odorant response varied greatly as shown, from 4.3 to 10.9 s. (*A*) Larger odorant responses taken from three different cells. The top trace was taken from a cell that had been previously stimulated by odorants, which may account for the extensive noise throughout the trace. These traces were taken at pipette potentials of +38 mV (*top*), 10 mV (*middle*) and 24 mV (*bottom*). (*B*) A plot of net odorant-induced current against pipette potential for a different cell (#191b). The slope conductance was estimated from the slope of the graph to be 83 pS and the net current for a pipette potential of zero was -0.60 pA. The cell potential, V_{cell}, when $V_p = 0$, was estimated to be -39 mV (for $R_p/R_o = 10$).

and the reciprocal of the seal resistance, assumed not to be affected by the odorant, as G_s and given by:

$$G_s \equiv 1/R_s \quad (12)$$

then the difference in G_{cell} due to odorant application will be given (see Appendix A) by:

$$\Delta G_{cell} = G^*_{cell} - G_{cell} = 1/R^*_t - 1/R_t = (-d\Delta I_p/dV_p) \quad (13)$$

since the seal resistance term, $1/R_s$, will cancel out.

The average odorant-induced conductance increase across the cell and patch in the same four patches varied between 14.6 and 83.5 pS, with a mean of 35.8 ± 16.2 pS (Table 2). A representative current-voltage relationship of an odorant-induced conductance in one cell is shown in Fig. 2 *B*. Since the input resistance of these cells is so high, it might have been expected that there would be a contribution

TABLE 2 Odorant perfusion experiments in GMR solutions containing 2 mM Ca^{2+} and 1 mM Mg^{2+}

	Control resting situation					Odorant perfusion situation									
Cell No.	$I_p(0)$	V_{cell} (mV; α = 10)	V_{cell} (mV; α = 100)	G_{cell} (pS)	R_t (GΩ)	ΔG_{cell} (pS)	$\Delta I_p(0)$ (pA)	G_{co}/G_o	$G_{co}/G_o^{\#}$	V_{cell}^* (mV; α = 10)	$V_{cell}^{\#}$ (mV; α = 10)	V_{cell}^* (mV; α = 100)	G_{cp}/G_p (α = 10)	$G_{cp}/G_p^{\#}$ (α = 10)	G_{cp}/G_p (α = 100)
181a	−9.40	−59.1	−64.4	144.7	0.87	14.60	−0.82	0.01	0.02	−57.8	−57.9	−63.5	0.11	0.11	0.10
191b	−8.71	−59.1	−64.4	134.0	2.33	83.47	−0.60	0.52	0.84	−38.6	−39.3	−42.3	0.63	0.60	0.62
241a	−1.79	−59.1	−64.4	27.5	5.68	28.18	−1.02	0.29	0.43	−43.2	−43.9	−49.6	1.15	1.11	1.04
241b	−1.11	−59.1	−64.4	17.1	6.08	16.92	−0.64	0.26	0.38	−44.1	−44.7	−50.7	1.11	1.08	1.00
Avr	−5.25	−59.1	−64.4	80.8	3.74	35.79	−0.77	0.27	0.42	−45.9	−46.5	−51.5	0.75	0.73	0.69
SEM	2.20	0	0	33.9	1.27	16.17	0.10	0.10	0.17	4.140	4.0	4.4	0.24	0.24	0.22

*These are the results of an analysis of intact patch measurements before and during odorant perfusion, using the equations derived in Appendix A.
$^{\#}E_{co}/E_o$ = 0.25.

to the recorded current from channel openings in the rest-of-cell (see discussion in Appendix B; Eq. B4). However, calculations for these cells suggested that such a contribution would be very small. In two of the cell-attached patches the noise increase was small enough to measure the apparent single-channel slope conductance as a function of pipette potential. A set of current traces is shown for one cell in Fig. 3 *A* and a plot of single channel current against pipette potential is shown in Fig. 3 *B*. The mean value of the apparent single-channel conductance (γ_p') was 15.8 ± 1.2 pS (n = 2) and it should be noted that there were no divalent ions in the patch pipette solution.

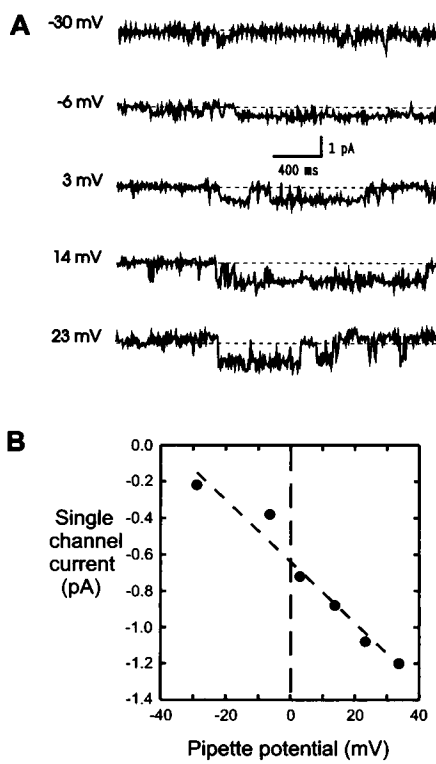

FIGURE 3 (*A*) Short segments of current traces taken at different pipette potentials on the same ORN during a period of odorant stimulation, for a cell (#241b) bathed in GMR solution, containing 2 mM Ca^{2+}, 1 mM Mg^{2+}. Single-channel activity can readily be resolved at each potential. (*B*) A plot of single channel current against pipette potential. The single-channel conductance was estimated from the slope of the graph to equal 17 pS and the net current for a pipette potential of zero was −0.64 pA. The cell potential when V_p = 0 was estimated to be −44 mV (for an estimate of R_p/R_o = 10).

Assuming that $R_p \gg R_o$, it is shown in Appendix B that, whereas currents due to single channels opening in the membrane patch will only be slightly reduced in magnitude, currents due to single channels opening in the rest-of-cell will be radically reduced. The actual value of the single-channel conductance of channels in the patch (γ_p) may be slightly larger than the apparent value (γ_p'), being given in Appendix B (Eq. B13), by:

$$\gamma_p \approx \gamma_p' (1 + \delta)^2 \tag{14}$$

provided $\gamma_p \ll G_o^*$ and where $\delta = G_p^*/G_o^*$, with G_p^* and G_o^* representing the values of the conductance across the patch and rest-of-cell in the presence of odorants. It would be expected that δ would be <0.1, so that at most the above figures would represent only a 21% underestimate of the conductance. The ratio of current due to multiple channel openings in the patch (expected to be a similar underestimate) compared to a single opening would be expected to be an accurate estimate of the number of open channels in the patch. Hence, an upper limit to the average number of open channels per patch was 35.8/15.8 ≈ 2.3.

An order of magnitude estimate of the maximum density of odorant-activated channels on the cell soma could be calculated from an estimate of the area (A) of the patch of membrane at the tip of the pipette. Assuming it to be intermediate between a hemisphere ($A = 2\pi r^2$) and a flat circle ($A = \pi r^2$) with diameter 2.5 μm, its area was estimated to be ~7.4 μm^2 to give an upper limit to the average channel density of ~0.3 channels opening per μm^2 on the soma. By comparison, Kurahashi and Kaneko (1993) estimated the CNG channel density on the soma of toad olfactory neurons to be approximately 6 per μm^2.

As indicated above, the opening of single channels in the rest-of-cell would only be seen as very small current deflections in the intact patch records. From Appendix B, it is shown that:

$$\gamma_o \approx \gamma_o'(1 + \delta)^2/\delta^2 \tag{15}$$

where γ_o' represents the apparent conductance of single channels opening in the rest-of-cell when measured across an intact patch, and γ_o represents their actual value. This means that when δ lies between 0.01 and 0.1, γ_o' will be only ~1/100-1/10,000 of the true value of γ_o.

Can we deduce any further information about the effect of the odorants on the cell parameters? In addition to the values of the reversal potential of the resting K^+ channels, we can make reasonable estimates of the ratio of the patch background resistance to the rest-of-cell resistance ($\alpha \equiv R_p/R_o$), and of the ratio of the reversal potentials of odorant-sensitive channels in the patch and the resting K^+ channels in the rest-of-cell (E_{co}/E_o). The value of α is likely to be between 10 and 100 (see earlier discussion) and for simplicity a value of 10 will be assumed in the text, although values of 5 and 100 are also included in Tables 2 and 3 to show the relative insensitivity of our calculations to changes in α over this range. If the patch contains only CNG cation channels, E_{co}/E_o should be close to 0. However, to allow for the possible presence of Ca^{2+}-activated chloride channels, calculations assuming an upper limit of 0.25 will also be included in Tables 2 and 3. Given these assumptions, we can estimate both the changes in cell potential due to the odorant action and even estimate the relative conductance changes in, and current components through, the patch and rest-of-cell membranes. We will see that some parameters are essentially independent of the value of E_{co}/E_o (see Tables 2 and 3), whereas others are very dependent on it.

Making use of the analysis in Appendix A, we can estimate these parameters as follows. The ratio of the conductance of the odorant-induced channels in the rest-of-cell, G_{co}, to the conductance of the rest-of-cell before odorant perfusion, G_o, can be shown to be given (see Eq. A45) by:

$$G_{co}/G_o = R_o/R_{co} = (1 - \theta)/[\theta - (E_{co}/E_o)] \qquad (16)$$

with $\theta = I_p(0)^* R^*_{cell}/E_o$, from Eq. A43.

As shown in Table 2, this relative increase in conductance in four cells was 0.27 ± 0.10 for $E_{co}/E_o = 0$ or 0.42 ± 0.17 for $E_{co}/E_o = 0.25$ (see Table 2). Both values are independent of the value of α. This represents a significant proportional increase in conductance of the rest-of-cell. Assuming $\alpha \gg 1$, we can estimate the initial resting potential of the cell (V_{cell}), in the absence of odorants, from:

$$V_{cell} = I_p(0) \times R_p \qquad (17)$$

It is now possible to completely describe the electrical parameters of the cell and patch in the presence and absence of odorants as follows (see Table 2 and also Appendix A). Assuming $\alpha = 10$ from Eqs. 1–5 and Eq. 16, $R_p = 24.8 \pm 11.3$ GΩ and $R_o = 2.48 \pm 1.1$ GΩ and from Eq. 17, $V_{cell} = -59.1$ mV. In the presence of odorant perfusion, the final cell voltage (V^*_{cell}) for a pipette voltage of 0 mV depolarizes to −45.9 ± 4.1 mV, the amount of depolarization (~13 mV) being only weakly dependent on α and essentially independent of the ratio of E_{co}/E_o (Table 2). The situation will be illustrated later in Fig. 6.

As seen in Table 2, the final cell potential and the ratio of conductances in the patch, G_{cp}/G_p, are both fairly insensitive to the value of E_{co}/E_o, although, in contrast and as expected, the value of G_{co}/G_o is very dependent on it. We have also shown that the patch conductance is almost doubled ($G_{cp}/G_p = 0.75 \pm 0.24$), that there is only a relatively small depolarization of the cell compared to the effect of high KCl perfusion, and that an average of ~2-3 channels are being opened in the patch with a single-channel conductance of 16 pS.

Effect of odorant application in low calcium solutions

Since the odorants used in this study have been shown to selectively stimulate the production of cAMP, the two conductances most likely to be stimulated in mammalian olfactory receptor neurons are the cyclic nucleotide-gated (CNG) cation channels and Ca^{2+}-activated Cl^- channels. It is well known that physiological concentrations of extracellular Ca^{2+} and Mg^{2+} potently inhibit the olfactory CNG cation channels (Zufall and Firestein, 1993; Kleene, 1995), which would in turn preclude activation of the Ca^{2+}-activated Cl^- channels in the patch. We therefore investigated whether extracellular Ca^{2+} and Mg^{2+} were significantly inhibiting the odorant response. In these experiments, Mg^{2+} ions were omitted from the bathing solution and the extracellular Ca^{2+} lowered from 2 to 0.25 mM. The composition of the pipette

TABLE 3 Odorant perfusion experiments in low Ca^{2+} solutions, with 0.25 mM [Ca^{2+}]

	Control resting situation					Odorant perfusion situation									
Cell No.	$I_p(0)$	V_{cell} (mV; α = 10)	V_{cell} (mV; α = 100)	G_{cell} (pS)	R_t (GΩ)	ΔG_{cell} (pS)	$\Delta I_p(0)$ (pA)	G_{co}/G_o	$G_{co}/G_o^{\#}$	V_{cell}^* (mV; α = 10)	$V_{cell}^{\#}$ (mV; α = 10)	V_{cell}^* (mV; α = 100)	G_{cp}/G_p (α = 10)	$G_{cp}/G_p^{\#}$ (α = 10)	G_{cp}/G_p (α = 100)
222a	−58.9	−59.1	−64.4	905.5	0.58	169.3	20.2	0.81	1.47	−33.8	−34.4	−35.7	0.15	0.13	0.18
252d	−13.8	−59.1	−64.4	212.9	2.77	35.80	0.17	0.18	0.26	−50.0	−50.3	−54.4	0.17	0.16	0.17
252f	−0.9	−59.1	−64.4	13.8	10.16	141.0	−5.14	0.67	1.14	−15.2	−20.5	−36.4	25.1	18.4	10.9
Avr	−24.5	−59.1	−64.4	377.4	4.50	115.3	5.08	0.55	0.96	−33.0	−35.1	−42.2	8.46	6.2	3.7
SEM	17.6	0	0	270.2	2.90	40.62	7.7	0.19	0.36	10.1	8.6	6.1	8.31	6.1	3.6

*These are the results of an analysis of intact patch measurements before and during odorant perfusion, using the equations derived in Appendix A.
$^{\#}E_{co}/E_o = 0.25$.

solution was not changed. Under such ionic conditions, odorant responses were observed in 6 of 16 cells. In five of these cells, odorants induced an increase in noise and an outward current across the patch into the pipette at negative pipette potentials. Examples of such a response from one cell is shown in Fig. 4 *A* and a sample current-voltage relationship for an odorant-induced conductance increase is shown in Fig. 4 *B*. The following results are based on current-voltage relationships recorded from three cells.

Although there was significant variability in measurements from cells maintained under these conditions, the net currents were still described by Eq. 18, but now with $\Delta I_p(0) = +5.1 \pm 7.7$ pA and the increase in cell conductance, ΔG_{cell}, of 115 ± 41 pS. The relative increase in conductance of the rest-of-cell (G_{co}/G_o) was 0.55 ± 0.19. Following the analysis outlined in the previous section, the cell parameters were determined as follows (see Table 3 and also Appendix A).

Before application of odorants, with $\alpha = 10$, from Eqs. 1–5 and Eq. 18, $R_p = 23.6 \pm 21.0$ GΩ and $R_o = 2.36 \pm 2.1$ GΩ and from Eq. 17, $V_{cell} = -59.1$ mV. In response to odorant stimulation, there was an increase in conductance, G_{cell}, from 377 to 492 pS. The ratio of odorant induced conductance/resting conductance in the rest-of-cell, G_{co}/G_o, was 0.55 ± 0.19 in comparison to a ratio in the patch, G_{cp}/G_p, of 8.5 ± 8.3. Changing the value of α to 100 did not alter the value of G_{co}/G_o, but did change the value of G_{cp}/G_p to 3.7 ± 3.5. The final cell voltage for a pipette voltage of 0 mV depolarized from −59.1 mV to -33.0 ± 10.1 mV in the presence of odorants for $\alpha = 10$, and from −64.4 mV to -42.2 ± 6.1 mV for $\alpha = 100$. Thus, the depolarization was 26 mV for $\alpha = 10$ and 22 mV for $\alpha = 100$. The whole situation will be illustrated later in Fig. 7.

As we can see from Table 3, there is now a greater odorant-induced depolarization and a greater increase in total conductance across the cell in the absence of physiological concentrations of Ca^{2+} and Mg^{2+}. Hence, the conductance increase is most likely due to reduced channel block by Ca^{2+} and Mg^{2+}.

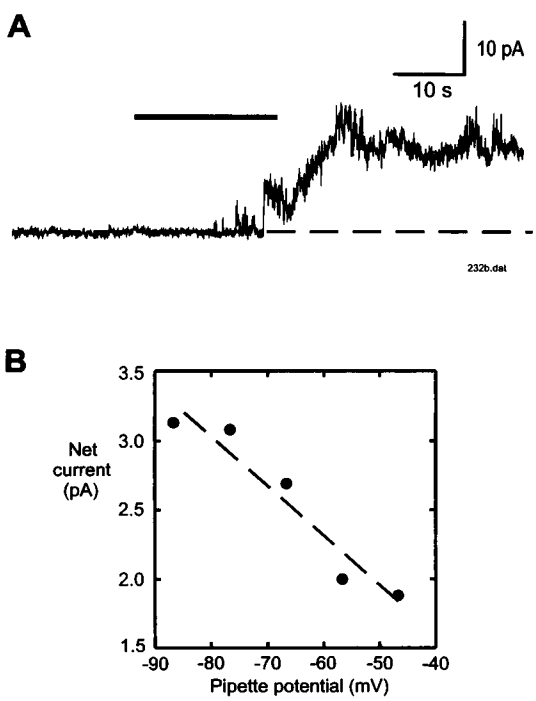

FIGURE 4 An odorant response for a cell in a low [Ca^{2+}] bath solution, containing 0.25 mM Ca^{2+} and 0 Mg^{2+}. (*A*) At a pipette potential of −62 mV in this cell, a 20-s application of odorants elicited a large increase in noise. Given such a pipette potential the resultant outward current across the patch into the pipette was much greater than when $V_p = 0$. (*B*) The net peak odorant-induced current, as a result of the opening of a few channels in the membrane patch, has been plotted against pipette potential for another cell in the same solution, and its slope conductance was estimated to equal 36 pS.

Effects of repeated odorant applications

With this intact patch configuration, subsequent odorant applications seemed to produce minimal changes in odorant response over a limited number (four or five) of applications, particularly with the higher divalent ions present. For example, in the case of Cell 241a (Table 2), a comparison of the response between the first and fourth odorant application at the same pipette potential only decreased by 5%. In some cases the first four or five odorant applications seemed very consistent, but the subsequent response dropped radically (e.g., by >70%) and it was considered that this was more likely to be a loss of seal rather than a rundown of the odorant response per se, and the experiment was terminated and the last response ignored. In the case of the low calcium solutions, there was generally much greater noise and a prolongation of the response to each odorant application, which increased with subsequent odorant applications and tended to result in the records becoming unusable after about four or five applications.

DISCUSSION

In this paper we have explored the possibility of using the intact patch configuration to monitor the responses of small olfactory neurons to stimulation by odorants and a high K^+ solution. To fully interpret our results and correctly deduce the changes in cellular parameters, given the complex electrical circuit of patch and rest-of-cell, a full analysis has been developed to account for the effects of stimuli that induce either depolarization or the opening of ion channels in the patch or rest-of-cell. Full derivations are given in Appendices A and B, and these have general applicability to any similar such conductance changes for high-input resistance cells monitored in the intact patch configuration.

We found that the application of a high K^+ solution *reduced the inward current* from the pipette into the cell, *equivalent to an additional outward component of current*, without any significant increase in current noise (Fig. 1 *B*). We have shown that this effect is due simply to the depolarization of the cell, thereby reducing the current flow from the pipette into the cell. A diagrammatical representation of

this situation is shown in Fig. 5. The magnitude of the depolarization depends on the relative resistances of the patch and the rest-of-cell. Assuming reversal potentials for the resting K^+ channels in the rest-of-cell and the patch of -65 mV and 0 mV, respectively, and a resistance ratio of patch to rest-of-cell (α) of 10, the resting potential of the cell with $V_p = 0$ was shown to be -59 mV (Table 1). Increasing external $[K^+]$ would be expected to decrease the reversal potential of the channels in the rest-of-cell to ~ -7 mV, and the cell membrane potential to -12 mV (or -13 mV for $\alpha = 100$), thus reducing the magnitude of the pipette current, as observed experimentally. The estimated change in reversal potential, ΔE_o, was 52 ± 10 mV. This value was independent of α and agreed very well with the theoretical prediction of 59 mV, thus establishing the validity of this approach for estimating membrane potential changes.

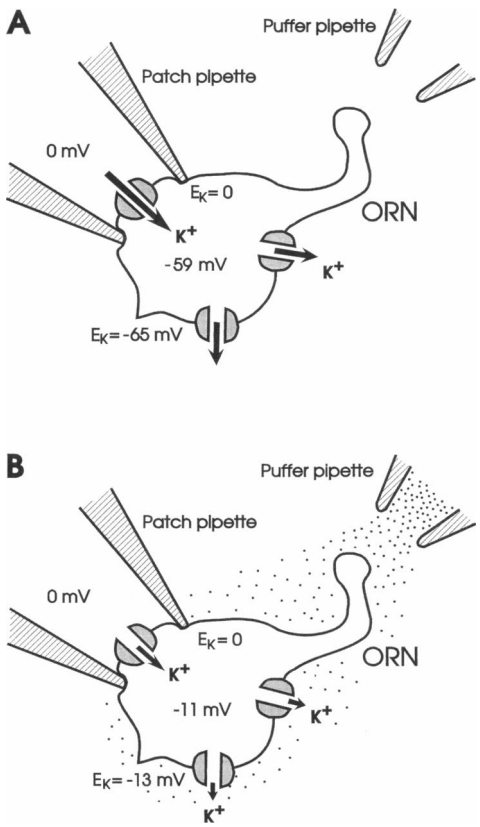

FIGURE 5 A diagram showing the effect of KCl application onto a cell-attached ORN. The channels shown are K^+ channels that are open at rest and confer onto the cell its high resting K^+ permeability. In (*A*) before odorant application, with a pipette potential of 0 mV, the cell membrane potential is estimated to be ~ -59 mV (assuming $R_p/R_o = 10$; see also Table 1). Since the pipette contained 135 mM K^+ and ORNs are known to have a high intracellular K^+ concentration similar to this value, the reversal potential for the K^+ channels, E_K, in the patch can be assumed to be close to zero and that for the rest-of-cell ~ -65 mV. In (*B*), application of the high K^+ solution from a puffer pipette resulted in a depolarization of the cell from -59 mV to -11 mV, a reduction in driving force for K^+ to enter the cell across the patch, and hence also a reduction in inward current across the cell [shown by the reduced arrow size between panels (*A*) and (*B*)], equivalent to a net outward odorant-induced current across the patch. In each panel, the lengths of the arrows (or their sums) are intended to be approximately proportional to the amplitudes of the current components.

The absence of any change in current noise or increase in conductance during K^+ application indicated that the depolarization did not activate voltage-gated channels in the patch. This was expected, as voltage-gated Na^+ and K^+ channels in dissociated rat olfactory neurons have an extremely negative voltage-dependence (Lynch and Barry, 1991a, 1991b; Rajendra et al., 1992) and would have been completely inactivated at the depolarized membrane potential of ~ -59 to -64 mV set by the specially elevated $[K^+]_o$ of the bathing solution.

Responses to a cocktail of odorants were observed in $\sim$17% (5 of 30) cells. *In the presence of odorants there was an increase in the current* from the pipette across the patch into the cell, *equivalent to an additional inward component of current* from pipette into cell. The estimated depolarization was much less than for the high K^+ solution, with the estimated cell potential changing from -59 mV to -46 ± 4 mV for $\alpha = 10$ (Table 2). As demonstrated by the analysis in Appendix B, channel activity due to channels opening in the patch should be reasonably faithfully reproduced by the pipette current, with only slight reductions in magnitude, whereas channel activity in the rest-of-cell should be radically diminished in magnitude by a factor between 100 to 10,000. As depicted in Fig. 6, the effect of odorants was modeled by a current flux into the cell from the pipette with odorant-activated current also entering across the rest-of-cell from the bath, and a subsequent cellular depolarization. The summed arrow lengths are intended to be approximately proportional to the main current components through the channels, without attempting to quantify the relative contributions of Cl^- and cation-selective CNG channels.

The odorant-induced channels in the patch were most likely to be CNG channels for several reasons. Firstly, we used only odorants known to stimulate the cAMP second messenger pathway. Secondly, since the pipette contained no divalent cations, they were unlikely to have been IP_3-gated channels. Furthermore, the single-channel conductance of 16 pS was similar to that expected for CNG channels (Frings et al., 1992). It is possible that Ca^{2+}-gated nonselective cation or Cl^- channels contributed to the current response, but these were unlikely to have been dominant since odorant-induced currents were dramatically larger when external Ca^{2+} was reduced. Currents activated by Ca^{2+} influx should have been reduced under these conditions. It should be noted that if odorant-activated channels were *only opened in the rest-of-cell* but *not in the patch*, the depolarization of the cell (due to current entering through the channels in the rest-of-cell membrane) would actually lead to *a reduction in the current leaving the pipette*, similar to the situation already seen for high KCl depolarization. However, CNG channels in the rest-of-cell were presumably strongly inhibited by divalent cations in the external solution (Zufall and Firestein, 1993; Kleene, 1995).

In this study, the latency of odorant-induced currents from commencement of the stimulus was 4–10 s, whereas

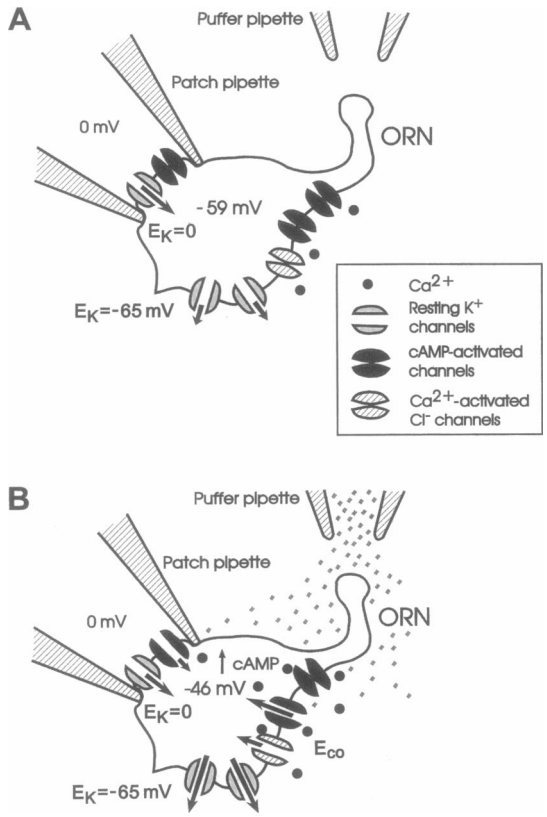

FIGURE 6 The effect of odorants on ORNs in a GMR bath solution, which contained 2 mM Ca^{2+} and 1 mM Mg^{2+}. The channels in black represent cationic CNG channels and those in gray the resting K^+-selective channels. (*A*) In the resting situation in the absence of odorants and with a pipette potential of 0 mV, the estimated membrane potential is −59 mV (for R_p/R_o = 10, as assumed for figure; see also Table 2). (*B*) Odorants activate the cAMP second messenger system, opening CNG channels once cAMP has diffused from the cilia to the soma. External Ca^{2+} ions entering through the cAMP-activated channels are also able to open Cl^- channels with a resultant efflux of Cl^- from the cell and increased inward depolarizing current. In addition, external divalent cations (both Ca^{2+} and Mg^{2+}) are also able to block some of the CNG channels, preventing too great a cell depolarization. However, the CNG channels in the patch are not directly exposed to external divalent cations, but are still activated by cAMP and produce a net inward current from the pipette when V_p = 0. This occurs in spite of the depolarization of the cell (to ~−46 mV for R_p/R_o = 10; see also Table 2) that results from the opening of the cAMP-gated channels in the rest-of-cell and its resulting inward movement of cations into the cell through them. The increased current across the patch results directly from the opening of cAMP-gated channels in the membrane patch (see figure). The lengths of the arrows (or their sums) are intended to be approximately proportional to the amplitudes of the main current components, without being too precise about the relative contributions of the cAMP-gated channels and the Ca^{2+}-activated Cl^- channels. E_{co} is intended to represent the combined reversal potential of both the cAMP-activated channels and the Ca^{2+}-activated Cl^- channels, and the legend is intended to apply to both panels.

whole-cell studies have shown latencies of several hundred milliseconds (Kurahashi, 1989; Firestein et al., 1990; Lowe and Gold, 1993). This discrepancy can be explained by the fact that in the present study we used cell-attached patches from the soma. Since most of the transduction machinery is known to be concentrated in the cilia, it is likely that second messengers are produced there and may require several seconds to diffuse to the somatic membrane. In both of the above studies the patch-clamp configuration being whole-cell, the measurements would tend to reflect conductance changes throughout the cell, whereas in the present study they primarily reflect the conductance changes in the membrane patch. If these present measurements are giving a better indication of the time for cAMP to diffuse from the cilia and dendritic region to the membrane patch, this would suggest a much lower diffusion coefficient. Part of the discrepancy could also lie in species differences with perhaps more effective slowing of diffusion by binding in the case of these mammalian ORNs than in the larger amphibian ORNs in the above cited studies. Future experiments combining the very elegant methodology of Lowe and Gold (1993) with intact patch measurements may help to resolve these differences.

Reducing the concentration of divalent cations in the bath solution resulted in a net *outward current across the patch for* V_p = 0 during odorant application, together with an associated increase in current noise. It was also considered that this decrease in divalent ion concentration would have been likely to make the cells more leaky and possibly more depolarized. However, to make some estimates of cell parameters, it was still assumed that the cell was predominantly permeable to K^+ in its resting state, so that the value of $E_o = E_K$ would still be ~−65 mV, although the cell potential (V_{cell}) could still be somewhat more depolarized than this.

However, in the low divalent cation solution there was a greater overall conductance for the patch and cell and a greater magnitude of $I_p(0)$, the patch current at zero pipette potential, before odorant application. Under these conditions, the duration of the odorant response in some cells was prolonged to values ~20 s, which was probably due to a reduced effectiveness of Ca^{2+}-dependent inactivation mechanisms (Kurahashi and Shibuya, 1990). However, the reversal in direction of the odorant-induced current suggests that channels in the rest-of-cell were now dominating the response. This is to be expected if the low divalent solution were unblocking odorant-sensitive channels in the rest-of-cell. These responses were probably also due to CNG channels that are strongly inhibited by physiological external divalent ion concentrations (Zufall and Firestein, 1993; Kleene, 1995). As explained above, this increase was unlikely to have been due to Ca^{2+}-gated chloride or cation channels, as these should have predominated at higher external [Ca^{2+}].

These results and their implications can be understood by inspection of Table 3 and Fig. 7, which depicts the cell-attached configuration with cAMP-gated channels in the patch. Again, the summed arrow lengths are intended to be approximately proportional (although at half the scale of those in Figs. 5 and 6) to the main current components through the channels, without attempting to quantify the relative contributions of Cl^- and the now more predominant cation-selective CNG channels. As shown in Fig. 7*A*, the

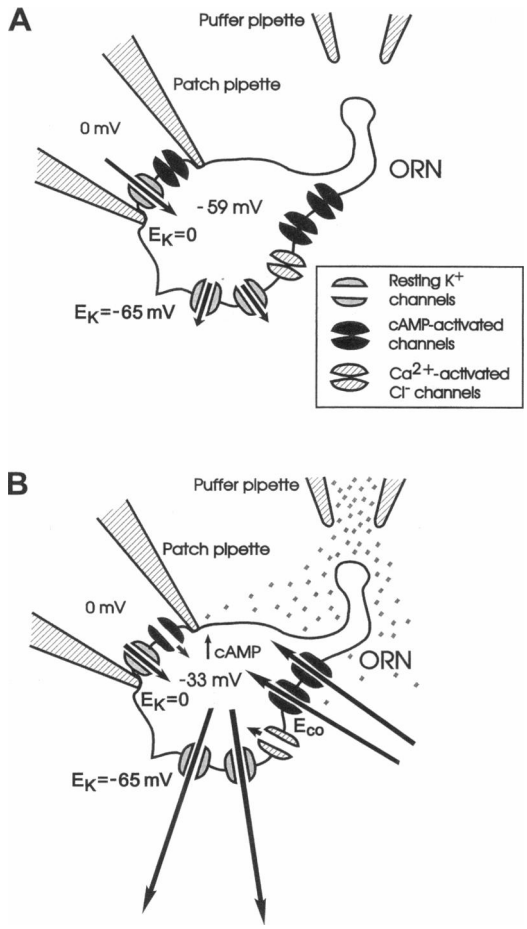

FIGURE 7 The effect of odorants on ORNs in a low Ca^{2+} bath solution, containing "0" Mg^{2+} and 0.25 mM Ca^{2+}. (*A*) When the pipette potential is 0 mV, the cell potential is expected to be −59 mV. (for R_p/R_o = 10, as assumed for figure; or −64 mV for R_p/R_o = 100). The current entering the cell across the patch must then flow out through channels in the rest-of-cell. (*B*) Application of odorants is expected to result in cAMP production within the cell and activation of CNG channels. The low divalent cation concentration in the bath is expected to be insufficient to block any CNG channels located on the cell membrane, so that the cell will now be depolarized to a much greater extent by odorants than was the case in Fig. 6. At V_p = 0, the greater membrane depolarization increases the outward driving force of K^+ across the rest-of-cell, which compensates for the inward current flowing through the CNG channels across the rest-of-cell. These effects, combined with the CNG channels opening in the patch, produced a reduction in the inward current across the patch, as indicated. Again, the lengths of the arrows (or their sums) are intended to be approximately proportional to the amplitudes of the main current components, without being too precise about the relative contributions of the cAMP-gated channels and the Ca^{2+}-activated Cl^- channels. However, because of the very large currents in this low $[Ca^{2+}]$ solution, the arrows have been drawn at half the scale of the arrows in Figs. 5 and 6. E_{co} is intended to represent the combined reversal potential of both the cAMP-activated channels and the Ca^{2+}-activated Cl^- channels, and the legend is intended to apply to both panels.

cell may initially be at ~−59 mV (α = 10; or −64 mV for α = 100; Table 3) with current entering the cell through the resting K^+ channels in the patch equaling that leaving through the larger number of K^+ channels in the rest-of-cell. When odorant activity results in an increase in cAMP within the cell, the cell will tend to be much more depolarized by the opening of more CNG channels in the rest-of-cell than in the higher Ca^{2+} solution (see Fig. 7 *B* and compare Fig. 6 *B*). The increased inflow of current through these channels will be partly balanced by an increased outflow through the resting K^+ channels, due to the much greater depolarization of the cell, as indicated. Nevertheless, on average there was now a decrease in current through the CNG channels across the patch and into the cell for V_p = 0 (see Table 3). This represents a net odorant-induced outflow of current into the pipette. Subsequent activation of the Cl^- conductance in the rest-of-cell would increase the depolarization and tend to increase this response (the relative sizes of arrows through these two sets of channels in the figure is not meant to be quantitative). However, because of the low external Ca^{2+}, the increase in Ca^{2+}-activated Cl^- conductances may not be so large, and hence this may not make a very large contribution to the current.

The cell-attached configuration thus provides a method in which odorant responses can be detected without disrupting the olfactory transduction cascade. It would avoid the problem of rundown encountered in whole-cell records of the odorant response in amphibian ORNs (Kurahashi, 1989; Trotier, 1986). As mentioned earlier (Effects of repeated odorant applications), there appeared to be no significant rundown for the first four or five odorant applications, and subsequent sudden reduction in response seems more likely to have been due to a loss of pipette seal resistance. This technique also has the advantage that the extracellular composition of the solution adjacent to the membrane patch can be altered to enhance the conductance of the channels underlying the odorant response, thereby facilitating detection of the response itself. Given some assumptions, a considerable number of cell parameters can be evaluated.

Assumptions of the model and reliability of parameter estimates

To readily evaluate the above parameters, a number of very reasonable assumptions needed to be made. 1) It was assumed that the initial resting potential of the ORN was close to the K^+ equilibrium potential, E_K. Given the high K^+ permeability of typical ORNs at rest and the high value of $[K]_o$ of 10 mM in these experiments, this should be a most reasonable assumption. Even in low Ca^{2+} solutions, when the membrane conductance is somewhat higher, it will probably still be reasonably valid. 2) Given the symmetrical K^+ concentrations across the membrane patch, the assumptions that E_p and E_{cp} = 0 should be very reasonable indeed. 3) As may be seen from Table 1, for example, even over a wide range of ratios of patch to rest-of-cell resistance (α; for $\alpha \geq 10$) the changes in cell potential and increases in patch conductance due to odorant action are little affected (see earlier discussion and estimates of Lynch and Barry (1989). 4) Similarly, a contribution of calcium-activated Cl^- channels to the reversal potential of the combination of the two

channels, E_{co}, (expected to be close to 0 for cAMP channels alone) had very little effect on the above parameters.

The variability of the cell parameters in the tables and fairly high SEMs are most likely to reflect cell-to-cell differences. The consistent responses for multiple odorant applications (see earlier section) and the relative insensitivity of the major parameter values to the above assumptions suggest that for a given cell these deduced parameters are fairly reliable and that simply increasing the number of cells will reduce these SEMs. However, what is also clear is that if a cell can be serially exposed to different odorants, under the same perfusion conditions, the *changes in parameter values for these different odorants for the same cell should be highly significant.*

CONCLUSION

This intact-patch technique, therefore, together with the accompanying detailed analysis of the full electrical circuit of patch and rest-of-cell outlined in Appendices A and B, could be most useful in characterizing some of the features of cAMP and IP_3-gated channels in rat ORNs, as well as in monitoring how various odorants and neurotransmitters could modulate conductances in other cells. This technique would also be especially useful for comparing the response of the same cell to different odorants (or other agents) and hence in determining the relative response selectivity of cells.

This work was supported by the Australian Research Council.

APPENDIX A: DERIVATION OF INTACT PATCH CIRCUIT EQUATIONS FOR MONITORING OF EFFECTS OF KCl DEPOLARIZATION AND ODORANT EFFECTS

by Peter H. Barry

General detailed solution of intact patch circuit equations

Initially, the general case will be considered, which will allow for additional channels to open up both in the membrane patch and in the rest of the cell, the latter hereafter being referred to as "rest-of-cell." This will then be followed by the treatment of specific cases.

From Kirchhoff's rules, defining the potentials in the directions indicated by the arrows in Fig. A1, as the potential of the arrowhead with respect to the tail, and the current direction being positive for currents entering the cell across R_o and R_{co} and in the direction of I_p, this direction being indicated by the direction of the arrowheads.

At the membrane patch, if the current leaving the cell through open channels is I_c, that across the rest of the patch is I_r, and the total current entering the cell is I_m, then:

$$I_m = I_c + I_r \tag{A1}$$

and

$$V_{cell} - E_{cp} - I_c R_{cp} - V_p = 0 \tag{A2}$$

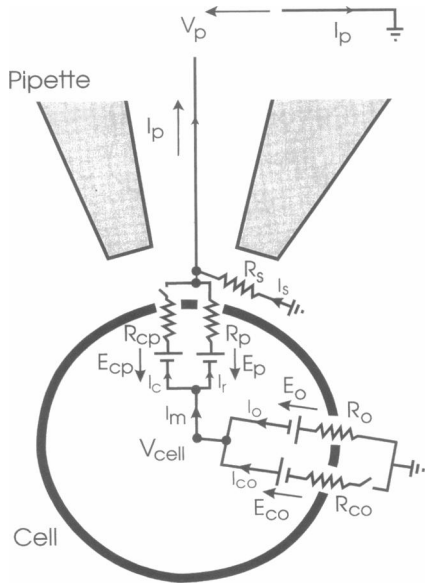

FIGURE A1 A diagram of the equivalent electrical circuit of a patch-clamp pipette in intact patch configuration with a small high-resistance cell. The circuit allows for the opening of separate channels in both the patch of membrane and the rest-of-cell. The electrical parameters are all defined in Appendix A.

Similarly,

$$V_{cell} - E_p - I_r R_p - V_p = 0 \tag{A3}$$

Hence,

$$I_c = (V_{cell} - E_{cp} - V_p)/R_{cp} \tag{A4}$$

$$I_r = (V_{cell} - E_p - V_p)/R_p \tag{A5}$$

Therefore:

$$I_m = [(V_{cell} - E_p - V_p)/R_p] + [(V_{cell} - E_{cp} - V_p)/R_{cp} \tag{A6}$$

In addition, across the seal resistance,

$$V_p + I_s R_s = 0 \tag{A7}$$

and

$$I_p = I_m + I_s \tag{A8}$$

so that

$$I_p = I_m - V_p/R_s \tag{A9}$$

Similarly, across the remainder of the cell:

$$V_{cell} - E_o + I_o R_o = 0 \tag{A10}$$

and

$$V_{cell} - E_{co} + I_{co} R_{co} = 0 \tag{A11}$$

with

$$I_o + I_{co} = I_m \tag{A12}$$

so that

$$I_m = [(E_o - V_{cell})/R_o] + [E_{co} - V_{cell})/R_{co}]] \tag{A13}$$

Rearranging Eqs. A6 and A13, we obtain:

$$I_m = [1/R_p + 1/R_{cp}]V_{cell} - [(E_p + V_p)/R_p] - [(E_{cp} + V_p)/R_{cp}] \quad (A14)$$

$$I_m = [(E_o/R_o) + (E_{co}/R_{co})] - [(1/R_o) + (1/R_{co})]V_{cell} \quad (A15)$$

Defining the total resistance across the membrane as R_p^*, in the presence of odorant-induced channels in the patch, then:

$$1/R_p^* = (1/R_p) + (1/R_{cp}) \quad (A16)$$

and the total resistance across the rest-of-cell as R_o^*, in the presence of odorant-induced channels in the rest-of-cell, then:

$$1/R_o^* = (1/R_o) + (1/R_{co}) \quad (A17)$$

From Eqs. A14 and A16:

$$V_{cell} = I_m R_p^* + [(E_p/R_p) + (E_{cp}/R_{cp})]R_p^* + V_p[(1/R_p) + (1/R_{cp})]R_p^* \quad (A18)$$

and from Eqs. A15 and A17,

$$V_{cell} = [(E_o/R_o) + (E_{co}/R_{co})]R_o^* - I_m R_o^* \quad (A19)$$

Hence,

$$I_m(R_o^* + R_p^*) = [(E_o/R_o) + (E_{co}/R_{co})]R_o^* - [(E_p/R_p) + (E_{cp}/R_{cp})]R_p^* - V_p \quad (A20)$$

Defining the total cell resistance in the presence of odorants as R_{cell}^* then:

$$R_{cell}^* = R_p^* + R_o^* \quad (A21)$$

and using Eq. A9, the general case for ionic channels opening on both the membrane patch and the rest-of-cell becomes:

$$I_p = [(E_o/R_o) + (E_{co}/R_{co})](R_o^*/R_{cell}^*) - [(E_p/R_p) + (E_{cp}/R_{cp})] \cdot (R_p^*/R_{cell}^*) - V_p[(1/R_{cell}^*) + (1/R_s)] \quad (A22)$$

where R_{cell}^* refers to the total cell resistance in the presence of these open channels.

We will now consider some special cases:

Case 1: Before odorants or KCl perfusion—both R_{co} and $R_{cp} \rightarrow \infty$

Hence R_p^* is replaced by R_p, R_o^* by R_o, and R_{cell}^* by $R_{cell} = R_o + R_p$ Therefore:

$$I_p = [(E_o - E_p)/(R_o + R_p)] - V_p\{[1/(R_o + R_p)] + [1/R_s]\} \quad (A23)$$

If $E_p = 0$, because $[K^+]_p = [K^+]_{cell}$, then

$$I_p = I_p(0) - V_p/R_t \quad (A24)$$

with

$$I_p(0) = E_o/R_{cell} \quad (A25)$$

where $I_p(0)$ represents the current when $V_p = 0$, and R_t, representing the total resistance of the cell, patch and seal, is defined by

$$1/R_t = [1/R_{cell}] + [1/R_s] \quad (A26)$$

with R_{cell} defined in turn by:

$$R_{cell} = R_o + R_p \quad (A27)$$

From Eq. A24, it may be seen that $R_t = -dV_p/dI_p$.

Case 2: After KCl perfusion—R_{co} and R_{cp} still $\rightarrow \infty$

Again, it will be assumed that $E_p = 0$, because $[K^+]_p = [K^+]_{cell}$. It will be assumed that both R_{co} and R_{cp} still $\rightarrow \infty$, that R_s remains unchanged, and that the effect of the high KCl is to simply allow for a change (depolarization) in E_o to go to E_o', and a possible change in R_o to go to R_o', so that R_{cell} changes to R_{cell}'. Thus we will have:

$$I_p = [E_o'/R_{cell}'] - V_p\{[1/R_{cell}'] + [1/R_s]\} \quad (A28)$$

with

$$R_{cell}' = R_o' + R_p' \quad (A29)$$

$$dI_p/dV_p = -([1/R_{cell}'] + [1/R_s]) \quad (A30)$$

and

$$I_p(0) = [E_o'/R_{cell}'] \quad (A31)$$

Alternatively, to a first approximation, from Eq. A26,

$$\Delta I_p(0) \approx [1/R_{cell}]\Delta E_o - (E_o/R_{cell}^2)\Delta R_{cell} \quad (A32)$$

so that

$$\Delta E_o \approx \Delta I_p(0)\, R_{cell} + (E_o/R_{cell})\Delta R_{cell} \quad (A33)$$

If $\Delta R_{cell} \approx 0$, then from Eq. A32,

$$\Delta E_o \approx \Delta I_p(0) R_{cell} \quad (A34)$$

Also, from the difference in slopes of pipette current, I_p, versus V_p, (high KCl perfusion minus control), the difference in total cell resistances can be obtained from:

$$(d\Delta I_p/dV_p) = (1/R_{cell}') - (1/R_{cell}) \quad (A35)$$

For estimates of changes in cell membrane potential, V_{cell}, see Section B following.

Case 3: After odorant perfusion

Again, it will be assumed that $E_p = 0$ and $E_{cp} = 0$, because $[K^+]_p = [K^+]_{cell}$. Then:

$$I_p^* = [(E_o/R_o) + (E_{co}/R_{co})](R_o^*/R_{cell}^*) - V_p[(1/R_{cell}^*) + (1/R_s)] \quad (A36)$$

with

$$R_{cell}^* = R_p^* + R_o^* \quad (A37)$$

with

$$1/R_o^* = (1/R_o) + (1/R_{co}) \quad (A38)$$

$$1/R_p^* = (1/R_p) + (1/R_{cp}) \quad (A39)$$

As with the high KCl perfusion case and from Eq. A36, from the difference in slopes of pipette currents, I_p^* and I_p, versus V_p, (odorant perfusion values minus control), the difference in total cell resistances can be obtained from:

$$(d\Delta I_p/dV_p) = (1/R_{cell}^*) - (1/R_{cell}) \quad (A40)$$

This value should now represent the total increase in conductance due to channels opening in response to odorants, and should give an indication of how many channels have opened up.

It seems likely that E_{co} may lie between 0 mV and −65 mV, depending on the relative contribution of the cAMP induced cation channels (E_{co} = 0 mV; fairly nonselective with approximately symmetrical total concentrations of cations), and the contribution of the Ca^{2+}-gated Cl^- channels ($E_{co} \sim -65$ mV). Hence, from Eq. A36,

$$I_p(0)^* = [(E_o/R_o) + (E_{co}/R_{co})][(R_o R_{co})/(R_o + R_{co})]/R^*_{cell} \quad (A41)$$

since from Eq. A38,

$$R_{to} = (R_o R_{co})/(R_o + R_{co}) \quad (A42)$$

Thus,

$$I_p(0)^* R^*_{cell}/E_o \equiv \theta = [1 + \beta(E_{co}/E_o)]/(\beta + 1) \quad (A43)$$

where

$$\beta \equiv R_o/R_{co} \quad (A44)$$

and so,

$$\beta = R_o/R_{co} = G_{co}/G_o = (1 - \theta)/[\theta - (E_{co}/E_o)] \quad (A45)$$

with $\theta = I_p(0)^* R^*_{cell}/E_o$, from Eq. A43.

Assuming a value of E_{co}/E_o, Eq. A45 will enable us to determine the relative conductance of the odorant-induced channels compared to the original conductance of the rest-of-cell membrane.

Estimation of approximate changes in cell voltage, V_{cell}

To estimate the changes in cell voltage under different conditions, a few reasonable assumptions will have to be made.

First of all, it will be assumed that, given the symmetrical K^+ concentrations across the membrane patch, the potentials $E_p = E_{cp} = 0$.

From Eq. A6, it may be seen that, in general, when $V_p = 0$, $I_m = I_p(0)$. Thus,

$$I_p(0) = V_{cell}[(1/R_p) + (1/R_{cp})] \quad (A46)$$

Case 1: Cell voltage changes before KCl or odorant application

Before application of any odorant, $1/R_{cp} \rightarrow 0$, so that Eq. A46 simplifies to:

$$I_p(0) = V_{cell}/R_p \quad (A47)$$

and,

$$V_{cell} = I_p(0) \times R_p \quad (A48)$$

It is also known that from Eq. A25

$$I_p(0) = E_o/R_{cell} \quad (A49)$$

where

$$R_{cell} = R_p + R_o \quad (A50)$$

The only problem is that of determining the value of R_p. If we make the following definition, that

$$R_p/R_o \equiv \alpha \quad (A51)$$

then from Eqs. A50 and A51

$$R_p = [\alpha/(1 + \alpha)]R_{cell} \quad (A52)$$

From Eqs. A48, A49, and A52

$$V_{cell} = [\alpha/(1 + \alpha)]E_o \quad (A53)$$

If now it is assumed, as is reasonable, based on relative areas (e.g., Lynch and Barry, 1989), $\alpha \gg 1$ (e.g., $\alpha \geq 10$), then the total resistance across the patch and cell will be dominated by the resistance across the patch and $R_p \approx R_{cell}$, and

$$V_{cell} = [\alpha/(1 + \alpha)]E_o \quad (A54)$$

For large values of α, $[\alpha/(1 + \alpha)] \rightarrow 1$. However, even if we consider the worst case and assume for an upper limit that $\alpha = 10$, then to a first fairly rough approximation $V_{cell} = (10/11)\ E_o \approx E_o$. For the analysis of the data in this paper, we will assume that $\alpha = 10$ and will calculate everything precisely.

Case 2: Cell voltage changes after KCl perfusion—R_{co} and R_{cp} still $\rightarrow \infty$

It would not be expected that the resistance across the patch would change, and so as before

$$V^*_{cell} = I_p(0)^* \times R^*_p = I_p(0)^* \times [\alpha^*/(1 + \alpha^*)]R^*_{cell} \quad (A55)$$

but where now the * refers to the new values of $I_p(0)$, α, R_{cell}, and V_{cell} in the presence of a high concentration of KCl perfusing the cell.

Case 3: Cell voltage changes after odorant perfusion

After odorant perfusion, odorant-induced channels would be expected to open up in both the membrane patch and also the rest-of-cell. Thus, following Eq. A46

$$I_p(0) = V_{cell}[(1/R_p) + (1/R_{cp})] = V_{cell}/R^*_p \quad (A56)$$

where R^*_p now represents the new resistance across the patch due to the new odorant-induced channels and is given by:

$$1/R^*_p = (1/R_p) + (1/R_{cp}) \quad (A57)$$

and across the rest-of-cell the new resistance R^*_o due to the original channels and the new odorant-induced channels will similarly be given by:

$$1/R^*_o = (1/R_o) + (1/R_{co}) \quad (A58)$$

As before,

$$R^*_{cell} = R^*_p + R^*_o \quad (A59)$$

If $R^*_p \gg R^*_o$, then $R^*_{cell} \approx R^*_p$ and $V_{cell} \approx I_p(0) \times R^*_{cell}$. For accurate results, we cannot make this simplification and have to proceed as follows:

With the information that we have already accumulated, we can estimate R_o/R_{co} from Eq. A45, based on some assumption about E_{co}. Since we have already determined R_o from our earlier measurement of R_p and the assumed value of α, we can now determine R_{co} and hence R^*_o from a rearrangement of Eq. A58 as:

$$R^*_o = R_o \times R_{co}/(R_o + R_{co}) \quad (A60)$$

Hence, from Eq. A60

$$R^*_p = R^*_{cell} - R^*_o \quad (A61)$$

From this value of R_p^* and our previous determination of R_p

$$R_{cp} = R_p^* \times R_p/(R_p - R_p^*) \tag{A62}$$

We now know R_o, R_p, R_{co}, and R_{cp}. We can also determine the membrane potential of the cell, V_{cell}, when $V_p = 0$ from Eq. A55 as:

$$V_{cell} = I_p(0) \times R_p^* \tag{A63}$$

In addition, from Eqs. A4, A5, A10, and A11 with $E_p = E_{cp} \approx 0$ and an estimate of E_{co}, we can determine the current components flowing through each of the resistances, using the following equations:

$$I_r = V_{cell}/R_{pc} \tag{A64}$$

$$I_c = V_{cell}/R_p \tag{A65}$$

$$I_o = (E_o - V_{cell})/R_o \tag{A66}$$

$$I_{co} = (E_{co} - V_{cell})/R_{co} \tag{A67}$$

In addition, α^*, the new ratio of patch to rest-of-cell resistance, will be given by:

$$\alpha^* = R_p^*/R_o^* = G_o^*/G_p^* = (G_o + G_{co})/(G_p + G_{cp}) \tag{A68}$$

If the increase in channel conductance were to be proportional to membrane area, then G_{co}/G_{cp} would also equal α and from Eq. A68, it may easily be shown that $\alpha^* = \alpha$. However, this need not be the case.

APPENDIX B: DERIVATION OF CORRECTIONS FOR SINGLE-CHANNEL CONDUCTANCE MEASUREMENTS FROM AN INTACT PATCH

by Peter H. Barry

Single-channel opening in the membrane patch

From Eq. A26, the apparent single-channel slope conductance, γ', will be given by:

$$\gamma_p' = -d/dV_p(\Delta I_p) = \{1/R_{cell}^*\} - \{1/R_{cell}^*\} \tag{B1}$$

Where R_{cell}^* represents the resistance across the cell and membrane patch at any time before the opening of a single channel, and $R_{cell}^{*\prime}$ represents its resistance when the channel is open.

Expanding in terms of R_o^* and R_p^*, the resistances across the rest-of-cell and membrane patch, with $R_p^{*\prime}$ being the patch resistance when the channel is open, we obtain:

$$\gamma_p' = \{1/[R_o^* + R_p^{*\prime}]\} - \{1/[R_o^* + R_p^*]\} \tag{B2}$$

Replacing the resistances with the appropriate conductances, G_o^* $(1/R_o^*)$ and G_p^* $(= 1/R_p^*)$, Eq. B2 becomes:

$$\gamma_p' = \{1/[(1/G_o^*) + 1/(G_p^* + \gamma_p)]\} - \{1/[(1/G_o^*) + 1/(G_p^*)]\} \tag{B3}$$

where γ_p is the actual conductance of the channel opening in the membrane patch. Hence:

$$\gamma_p' = \{G_o^*(G_p^* + \gamma_p)/(G_o^* + G_p^* + \gamma_p)\} - \{G_o^*G_p^*/(G_o^* + G_p^*)\} \tag{B4}$$

and so, dividing the numerator and denominator of the first term by $(G_o^* + G_p^*)$, we obtain:

$$\gamma_p' = \{G_o^*(G_p^* + \gamma_p)/[(G_o^* + G_p^*)(1 + \gamma_p/(G_o^* + G_p^*))]\} - \{G_o^*G_p^*/(G_o^* + G_p^*)\} \tag{B5}$$

Taking the first term of the Taylor expansion of $(1 + \gamma_p/(G_o^* + G_p^*))^{-1}$, assuming that $\gamma_p \ll (G_o^* + G_p^*)$, we obtain:

$$\gamma_p' \approx \{G_o^*(G_p^* + \gamma_p)(1 - \gamma_p/(G_o^* + G_p^*))/(G_o^* + G_p^*)\} - \{G_o^*G_p^*/(G_o^* + G_p^*)\} \tag{B6}$$

Hence,

$$\gamma_p' \approx G_o^*/(G_o^* + G_p^*)\{[(G_p^* + \gamma_p)(1 - \gamma_p/(G_o^* + G_p^*))] - G_p^*\} \tag{B7}$$

$$\gamma_p' \approx [G_o^*\gamma_p/(G_o^* + G_p^*)]\{(1 - (\gamma_p + G_p^*)/(G_o^* + G_p^*))\} \tag{B8}$$

Dividing each ratio through by G_o^*, this simplifies to:

$$\gamma_p' \approx [\gamma_p/(1 + \delta)][(1 - ((\gamma_p/G_o^*) + \delta)/(1 + \delta))] \tag{B9}$$

where

$$\delta \equiv G_p^*/G_o^* \tag{B10}$$

This then becomes:

$$\gamma_p' \approx \gamma_p[1 - (\gamma_p/G_o^*)]/(1 + \delta)^2 \tag{B11}$$

and so

$$\gamma_p \approx \gamma_p'(1 + \delta)^2/[1 - (\gamma_p/G_o^*)] \tag{B12}$$

If $\gamma_p/G_o^* \ll 1$, then Eq. B12 simplifies to:

$$\gamma_p \approx \gamma_p'(1 + \delta)^2 \tag{B13}$$

δ is probably fairly similar in value to $1/\alpha$ $[= 1/(G_o/G_p)]$. If $\delta = 1/10$, then the correction is $\gamma_p \approx 1.21\ \gamma_p'$; whereas, if $\delta = 1/100$, then the correction is $\gamma_p \approx 1.02\ \gamma_p'$.

Single-channel opening in the rest-of-cell

As before, from Eq. A26, the apparent single-channel slope conductance, γ_o', will be given by:

$$\gamma_o' = -d/dV_p(\Delta I_p) = \{1/R_{cell}^{*\prime}\} - \{1/R_{cell}^*\} \tag{B14}$$

where again, R_{cell}^* represents the resistance across the cell and membrane patch at any time before the opening of a single channel, and $R_{cell}^{*\prime}$ represents its resistance when the channel is open.

Expanding in terms of R_o^* and R_p^*, the resistances across the rest-of-cell and membrane patch, with $R_o^{*\prime}$ being the rest-of-cell resistance when the channel is open, we obtain:

$$\gamma_o' = \{1/[R_o^{*\prime} + R_p^*]\} - \{1/[R_o^* + R_p^*]\} \tag{B15}$$

Replacing the resistances with the appropriate conductances, G_o^* $(= 1/R_o^*)$ and G_p^* $(= 1/R_p^*)$, Eq. B15 becomes:

$$\gamma_o' = \{1/[(1/(G_o^* + \gamma_o) + 1/G_p^*]\} - \{1/[(1/G_o^*) + 1/(G_p^*)]\} \tag{B16}$$

where γ_o is the actual conductance of the channel opening in the rest-of-

cell membrane. Hence:

$$\gamma_o' = \{(G_o^* + \gamma_o)G_p^*/(G_o^* + G_p^* + \gamma_o)\} - \{G_o^*G_p^*/(G_o^* + G_p^*)\} \quad \text{(B17)}$$

and so, dividing the numerator and denominator of the first term by $(G_o^* + G_p^*)$, we obtain:

$$\gamma_o' = \{(G_o^* + \gamma_o)G_p^*/[(G_o^* + G_p^*)(1 + \gamma_o/(G_o^* + G_p^*))]\} - \{G_o^*G_p^*/(G_o^* + G_p^*)\} \quad \text{(B18)}$$

Taking the first term of the Taylor expansion of $(1 + \gamma_o/(G_o^* + G_p^*))^{-1}$, assuming that $\gamma_o \ll (G_o^* + G_p^*)$, we obtain:

$$\gamma_o' \approx \{(G_o^* + \gamma_p)G_p^*(1 - \gamma_o/(G_o^* + G_p^*))/(G_o^* + G_p^*)\} - \{G_o^*G_p^*/(G_o^* + G_p^*)\} \quad \text{(B19)}$$

Hence,

$$\gamma_o' \approx G_p^*/(G_o^* + G_p^*)\{[(G_o^* + \gamma_o)(1 - \gamma_o/(G_o^* + G_p^*))] - G_o^*\} \quad \text{(B20)}$$

$$\gamma_o' \approx [G_p^*\gamma_o/(G_o^* + G_p^*)]\{1 - (\gamma_o + G_o^*)/(G_o^* + G_p^*)\} \quad \text{(B21)}$$

Dividing each ratio through by G_o^*, this simplifies to:

$$\gamma_o' \approx [\delta\gamma_o/(1 + \delta)][(1 - ((\gamma_o/G_o^*) + 1)/(1 + \delta))] \quad \text{(B22)}$$

where again

$$\delta \equiv G_p^*/G_o^* \quad \text{(B23)}$$

This then becomes:

$$\gamma_o' \approx \delta\gamma_o[\delta - (\gamma_o/G_o^*)]/(1 + \delta)^2 \quad \text{(B24)}$$

and so

$$\gamma_o \approx \gamma_o'(1 + \delta)^2/\{\delta[\delta - (\gamma_o/G_o^*)]\} \quad \text{(B25)}$$

If $\gamma_o/G_o^* \ll 1$, then Eq. B12 simplifies to:

$$\gamma_o \approx \gamma_o'(1 + \delta)^2/\delta^2 \quad \text{(B26)}$$

remembering that δ is probably fairly similar in value to $1/\alpha(= 1/(G_o/G_p))$. If $\delta = 1/10$, then the correction is $\gamma_p \approx 121\ \gamma_p'$, where as if $\delta = 1/100$, then the correction is $\gamma_p \approx 10{,}200\gamma_p'$. This indicates that any single-channel current jumps measured in the intact patch configuration and due to channels opening up in the rest-of-cell are very radically reduced in magnitude.

REFERENCES

Ache, B. W., and A. Zhainazarov. 1995. Dual second-messenger pathways in olfactory transduction. *Curr. Opin. Neurobiol.* 5:461–466.

Barry, P. H. 1994. JPCalc, a software package for calculating liquid junction potential corrections in patch-clamp, intracellular, epithelial and bilayer measurements and for correcting junction potential measurements. *J. Neurosci. Meth.* 51:107–116.

Barry, P. H., and N. Quartararo. 1990. PNSCROLL, a software package for graphical interactive analysis of single-channel patch clamp currents and other binary file records under mouse control. *Comp. Biol. Med.* 20: 193–204.

Bezanilla, F. 1985. A high capacity data recording device based on a digital audio processor and a video cassette recorder. *Biophys. J.* 47:437–441.

Dionne, V. E., and A. E. Dubin. 1994. Transduction diversity in olfaction. *J. Exp. Biol.* 194:1–21.

Dubin, A. E., and V. E. Dionne. 1993. Modulation of Cl^-, K^+ and nonselective cation conductances by taurine in olfactory receptor neurons of the mudpuppy *necturus maculosis*. *J. Gen. Physiol.* 101: 469–485.

Dubin, A. E., and V. E. Dionne. 1994. Action potentials and chemosensitive conductances in the dendrites of olfactory neurons suggest new features for odor transduction. *J. Gen. Physiol.* 103:181–201.

Fadool, D. A., and B. W. Ache. 1992. Plasma membrane inositol 1,4,5-trisphosphate-activated channels mediate signal transduction in lobster olfactory receptor neurons. *Neuron.* 9:907–918.

Firestein, S., G. M. Shepherd, and F. S. Werblin. 1990. Time course of the membrane current underlying sensory transduction in salamander olfactory receptor neurons. *J. Physiol.* 430:135–158.

Frings, S., J. W. Lynch, and B. Lindemann. 1992. Properties of cyclic nucleotide-gated channels mediating olfactory transduction: activation, selectivity and blockage. *J. Gen. Physiol.* 100:45–67.

Frings, S., R. Seifert, M. Godde, and U. B. Kaupp. 1995. Profoundly different calcium permeation and blockage determine the specific function of distinct cyclic nucleotide-gated channels. *Neuron.* 15:169–179.

Hatt, H., and B. W. Ache. 1994. Cyclic nucleotide- and inositol phosphate-gated ion channels in lobster olfactory receptor neurons. *Proc. Natl. Acad. Sci. USA* 91:6264–6268.

Kleene, S. J. 1993. Origin of the chloride current in olfactory transduction. *Neuron.* 11:123–132.

Kleene, S. J. 1995. Block by external calcium and magnesium of the cyclic-nucleotide-activated current in olfactory cilia. *Neuroscience.* 66: 1001–1008.

Kurahashi, T. 1989. Activation by odorants of cation-selective conductance in the olfactory receptor cell isolated from the newt. *J. Physiol.* 419: 177–192.

Kurahashi, T., and A. Kaneko. 1993. Gating properties of the cAMP-gated channel in toad olfactory receptor cells. *J. Physiol.* 466:287–302.

Kurahashi, T., and T. Shibuya. 1990. Ca^{2+}-dependent adaptive properties in the solitary olfactory receptor cells of the newt. *Brain Res.* 515: 261–268.

Kurahashi, T., and K. W. Yau. 1993. Co-existence of cationic and chloride components in odorant-induced current of vertebrate olfactory receptor cells. *Nature.* 363:71–74.

Lowe, G., and G. H. Gold. 1993. Nonlinear amplification by calcium-dependent chloride channels in olfactory receptor cells. *Nature.* 366: 283–286.

Lowe, G., and G. H. Gold. 1995. Olfactory transduction is intrinsically noisy. *Proc. Natl. Acad. Sci. USA.* 92:7864–7868.

Lynch, J. W., and P. H. Barry. 1989. Action potentials initiated by single channels opening in a small neuron (rat olfactory receptor). *Biophys. J.* 55:755–768.

Lynch, J. W., and P. H. Barry. 1991a. Properties of transient K^+ currents and underlying single K^+ channels in rat olfactory receptor neurons. *J. Gen. Physiol.* 97:1043–1072.

Lynch, J. W., and P. H. Barry. 1991b. Inward rectification in rat olfactory receptor neurons. *Proc. R. Soc. Lond. Ser. B.* 243:149–153.

Morales, B., G. Ugatre, P. Labarca, and J. Bacigalupo. 1994. Inhibitory K^+ current activated by odorants in toad olfactory neurons. *Proc. R. Soc. Lond. Ser. B.* 257:235–242.

Nakamura, T., and G. H. Gold. 1987. A cyclic nucleotide-gated conductance in olfactory receptor cilia. *Nature.* 325:442–444.

Okada, Y., J. H. Teeter, and D. Restrepo. 1994. Inositol 1,4,5-trisphosphate-gated conductance in isolated rat olfactory neurons. *J. Neurophysiol.* 72:595–602.

Pace, U., E. Hansky, Y. Salomon, and D. Lancet. 1985. Odorant sensitive adenylate cyclase may mediate olfactory reception. *Nature.* 316: 255–258.

Pun, R. Y. K., S. J. Kleene, and R. C. Gesteland. 1994. Guanine nucleotides modulate steady-state inactivation of voltage-gated sodium channels in frog olfactory receptor neurons. *J. Membr. Biol.* 142:103–111.

Rajendra, S., J. W. Lynch, and P. H. Barry. 1992. An analysis of Na^+ currents in rat olfactory receptor neurons. *Pflügers Arch.* 420:342–346.

Reed, R. R. 1992. Signalling pathways in odorant detection. *Neuron.* 8:205–209.

Schild, D., and F. W. Lischka. 1994. Amiloride-insensitive cation conductance in *Xenopus laevis* olfactory neurons: a combined patch-clamp and calcium imaging analysis. *Biophys. J.* 66:299–304.

Schild, D., F. W. Lischka, and D. Restrepo. 1995. $InsP_3$ causes an increase in apical $[Ca^{2+}]_i$ by activating two distinct current components in vertebrate olfactory receptor cells. *J. Neurophysiol.* 73:862–866.

Trotier, D. 1986. A patch-clamp analysis of membrane currents in salamander olfactory receptor cells. *Pflügers Arch.* 407:589–595.

Zhainazarov, A. B., and B. W. Ache. 1995. Na^+-activated nonselective cation channels in primary olfactory neurons. *J. Neurophysiol.* 73: 1774–1781.

Zufall, F., and S. Firestein. 1993. Divalent cations block the cyclic nucleotide-gated channel of olfactory receptor neurons. *J. Neurophysiol.* 69:1758–1768.